Quantum Monte Carlo Method in the Steady State

A. Erpenbeck,[1] E. Gull,[1] and G. Cohen[2,3]
[1]Department of Physics, University of Michigan, Ann Arbor, Michigan 48109, USA
[2]The Raymond and Beverley Sackler Center for Computational Molecular and Materials Science, Tel Aviv University, Tel Aviv 6997801, Israel
[3]School of Chemistry, Tel Aviv University, Tel Aviv 6997801, Israel

(Received 19 July 2022; revised 7 December 2022; accepted 7 April 2023; published 2 May 2023)

We present a numerically exact steady-state inchworm Monte Carlo method for nonequilibrium quantum impurity models. Rather than propagating an initial state to long times, the method is directly formulated in the steady state. This eliminates any need to traverse the transient dynamics and grants access to a much larger range of parameter regimes at vastly reduced computational costs. We benchmark the method on equilibrium Green's functions of quantum dots in the noninteracting limit and in the unitary limit of the Kondo regime. We then consider correlated materials described with dynamical mean field theory and driven away from equilibrium by a bias voltage. We show that the response of a correlated material to a bias voltage differs qualitatively from the splitting of the Kondo resonance observed in bias-driven quantum dots.

DOI: 10.1103/PhysRevLett.130.186301

Introduction.—Nonequilibrium driving can have profound effects on strongly correlated materials. Experimental probes have revealed intricate phenomena ranging from electrically induced metal-insulator transitions [1–8] to metastable nonequilibrium states [9–12] and driven superconductivity [13–16]. The rich variety of electronic phases and their sensitive dependence on external fields makes the physics of driven correlated electron systems a promising basis for next-generation nanoscale electronics [17]. The theoretical description of such physics, however, remains a challenging task.

To study a strongly correlated system out of equilibrium, one may expose it to short external stimuli or quenches, after which time propagation can be probed. This is the guiding principle for pump-probe approaches [13,18–25]. Another strategy is driving the correlated material into a time-independent nonequilibrium steady state, e.g., by applying an external bias voltage or temperature gradient. This is the approach taken in transport experiments [3,26–31].

Theoretical methodologies for the accurate description of transport experiments should ideally (i) be able to describe all aspects of correlation physics without introducing spurious artifacts and (ii) be able to access the steady state. The development of numerically exact methods that meet these requirements is an active field of research [32–38]. Successful approaches have so far relied on time propagation from a tractable initial state [36–38]. This strategy may become challenging when targeting strongly correlated steady states, where coherence times can be orders of magnitude longer than the intrinsic timescales in the electronic Hamiltonian [39–41]. Since most numerically exact methods face an exponential scaling of computational cost with simulation time [42–50], numerically exact simulations of steady states for correlated systems are often prohibitively expensive.

In this Letter, we present a numerically exact algorithm, applicable to strongly correlated systems, that provides direct access to the nonequilibrium steady state of quantum impurity models without propagation from an initial state. The method is based on the inchworm quantum Monte Carlo (IQMC) method [51] and enables the investigation of steady states forming at timescales that are orders of magnitude longer than what is accessible by techniques based on direct time propagation.

We use the equilibrium Anderson impurity model to benchmark our method against analytical limits and state-of-the-art numerical methods. We then apply our method to correlated materials within the equilibrium dynamical mean-field theory (DMFT) framework [52], demonstrating that it can be used to obtain real frequency spectra without the need for analytical continuation [53,54]. Using nonequilibrium DMFT [55–57], we finally consider a strongly correlated material placed between two metallic leads and subjected to a bias voltage [56,58]. This setup bears resemblance to a quantum dot driven by a bias voltage, as considered by Meir *et al.* [59], where it was shown that the Kondo peak or Abrikosov-Suhl resonance can be split by the voltage [60–69]. We investigate the effect of nonequilibrium driving on the quasiparticle peak, which is the lattice counterpart of the Kondo effect in the strongly correlated metallic regime. There, we show that an analogous—though, intriguingly, more subtle—splitting occurs.

Inchworm Monte Carlo method in the steady state.—Consider a quantum impurity model described by the

Hamiltonian $H = H_I + H_B + H_{IB}$, consisting of an interacting impurity H_I, a noninteracting bath H_B, and the coupling or hybridization between them H_{IB}. The central object of our method is the restricted propagator between two times on opposite branches of the Keldysh contour, $\Phi^{\beta}_{\alpha}(t,t') = \mathrm{Tr}_B\{\rho_B\langle\alpha|e^{iHt}|\beta\rangle\langle\beta|e^{-iHt'}|\alpha\rangle\}$. Here, α and β are states in the impurity subspace, and α is the impurity's initial condition. ρ_B is the initial bath density matrix and Tr_B denotes a trace over the bath degrees of freedom. A detailed discussion of these propagators is given in Refs. [66,70].

We calculate the restricted propagators using an expansion in the impurity-bath hybridization H_{IB}. The resulting high-dimensional integral expression for $\Phi^{\beta}_{\alpha}(t,t')$ can be evaluated by means of Monte Carlo methods [71–74]. A direct summation of all contributions results in the dynamical sign problem, an exponential growth in the required computational resources with simulation time [40,66,71,72,75–77] that effectively limits this approach to short times. The dynamical sign problem can often be overcome by the IQMC method [51,78–82]. Instead of calculating the restricted propagator directly, the IQMC method makes optimal use of the information incorporated in short-time dynamics to construct more efficient expansions for longer times. However, as the IQMC method requires knowledge of restricted propagators at all previous times, the algorithm scales at least quadratically with simulation time.

For the purpose of this Letter, the established two-time IQMC scheme can be considered to be a map F_{inch}, from the set of known restricted propagators up to the times t_1 and t_2, to the restricted propagator at (slightly) larger times t and t', with $t_1 \le t$ and $t_2 \le t'$. This can be written as follows:

$$F_{\mathrm{inch}}\colon \{\Phi^{\beta}_{\alpha}(\tau,\tau')|\tau \le t_1, \tau' \le t_2\} \to \Phi^{\beta}_{\alpha}(t,t'). \quad (1)$$

As the map F_{inch} is expressed in terms of known propagators, only a subclass of the summands that would appear in a bare hybridization expansion need to be included; these contributions are referred to as *inchworm proper* [51,79,80]. We have reproduced the detailed derivation for this map F_{inch} together with a diagrammatic representation in the Supplemental Material [83]. The IQMC method uses the map F_{inch} to propagate the restricted propagator forward in time, sequentially increasing each of t and t' in a set of small steps until both are sufficiently large [51].

For the steady state, the propagator becomes characterized by two simplifying conditions. It is (i) independent of the impurity's initial condition α and (ii) invariant to propagation in the direction $t, t' \to t + \Delta t, t' + \Delta t$, or, equivalently, dependent only on the time difference $t - t'$ rather than on the explicit values of t and t'. We use these facts to formulate an IQMC method directly in the steady state, by explicitly seeking a solution of the form $\Phi^{\beta}_{\alpha}(t,t') = \Phi^{\beta}(t-t')$. From the previous discussion, it follows that a steady-state $\Phi^{\beta}(t-t')$ must be a fixed point of the IQMC procedure:

$$F_{\mathrm{inch}}\colon \{\Phi^{\beta}(t-t')\} \to \Phi^{\beta}(t-t'). \quad (2)$$

That is, given the exact propagator at *all* time differences, the IQMC method will generate the same propagator at *each* time difference. We use this property as a self-consistency condition. The construction of the IQMC map F_{inch}, the associated diagrammatic representation, and the notion of inchworm proper diagrams remain identical to the time-dependent IQMC scheme [51,78,79], which is outlined in the Supplemental Material [83]. Note that the self-consistency condition we described exists within the IQMC method, but not within the bare hybridization expansion [71–74], because in the IQMC method the restricted propagator for a given time is expressed in terms of restricted propagators at previous times.

In practice, we start the self-consistency cycle from some initial guess for $\Phi^{\beta}(t-t')$ (we used a low-order perturbative result) and iterate Eq. (2) until the last two results are indistinguishable to within some tolerance. We have included further details, an explicit example for this self-consistent cycle, and a discussion on the numerical scaling in the Supplemental Material [83].

Once $\Phi^{\beta}(t-t')$ is known, the steady-state Green's functions (GFs) are obtained from existing techniques [66,78]. In particular, we calculate the retarded steady-state GF, $G^{r}_{\sigma\sigma'}(\Delta t) = -i\theta(\Delta t)\langle d_{\sigma}(\Delta t)d^{\dagger}_{\sigma'}(0) + d^{\dagger}_{\sigma'}(0)d_{\sigma}(\Delta t)\rangle$. The spectral function is then given by the Fourier transform of the retarded GF, $A_{\sigma\sigma'}(\epsilon) = -\mathrm{Im}\{G^{r}_{\sigma\sigma'}(\epsilon)\}$.

Anderson impurity model.—We present results for the Anderson impurity model, $H_I = \sum_{\sigma}\epsilon_0 d^{\dagger}_{\sigma}d_{\sigma} + U d^{\dagger}_{\uparrow}d_{\uparrow}d^{\dagger}_{\downarrow}d_{\downarrow}$, $H_B = \sum_{\sigma k}\epsilon_k a^{\dagger}_{k\sigma}a_{k\sigma}$, and $H_{IB} = \sum_{l}\sum_{k\in l}\sum_{\sigma}(V_k a^{\dagger}_{k\sigma}d_{\sigma} + \mathrm{H.c.})$. Here, ϵ_0 is the on-site energy on the impurity and U is the Coulomb interaction strength. d_{σ} and $d^{\dagger}_{\sigma}$, respectively, are annihilation and creation operators with spin $\sigma \in \{\uparrow,\downarrow\}$ on the dot. $a_{k\sigma}$ and $a^{\dagger}_{k\sigma}$ are their counterparts on the bath orbitals with energy ϵ_k. The dot-bath coupling for bath ℓ is characterized by the coupling strength function $\Gamma_{\ell}(\epsilon) = 2\pi\sum_{k\in\ell}|V_k|^2\delta(\epsilon-\epsilon_k)$. $\Gamma_{\ell}(\epsilon)$ is used to model either leads or an effective DMFT bath, each of which is initially at equilibrium [56]. Applying different chemical potentials μ_{ℓ} to different leads ℓ generates nonequilibrium steady states. As we only consider spin-independent cases, spin indices will be suppressed henceforth.

Benchmark I: Resonant level model.—We consider the noninteracting limit $U = \epsilon_0 = 0$ at equilibrium coupled to a single bath. While this system is exactly solvable and the underlying physics is well established [84,85], it is a challenging benchmark for hybridization expansions. Figure 1 shows the retarded GF and the spectral function obtained from the steady-state IQMC method at different

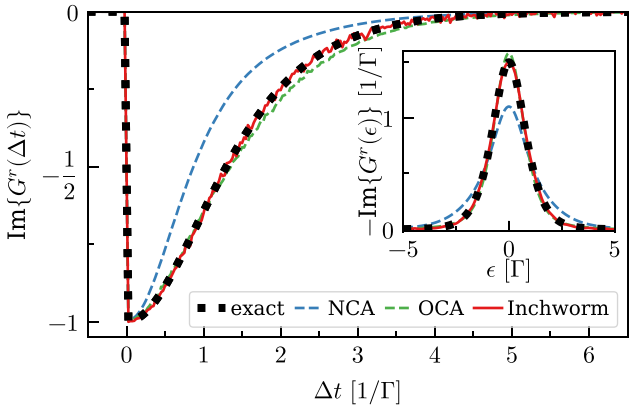

FIG. 1. Resonant level model. Steady-state retarded GF in real time and spectral function in real frequency (inset). Parameters are $\epsilon_0 = U = 0$ at temperature $T = \Gamma$, with the impurity coupled to a single, flat bath with bandwidth $\omega_c = 1.5\Gamma$ and cutoff width $1/\eta = \Gamma$: $\Gamma(\epsilon) = \Gamma/[(1 + e^{\eta[(\epsilon-\mu)-\omega_c]})(1 + e^{-\eta[(\epsilon-\mu)+\omega_c]})]$ and $\mu = 0$. The IQMC scheme converges at order 4 (6) for the propagator (GF).

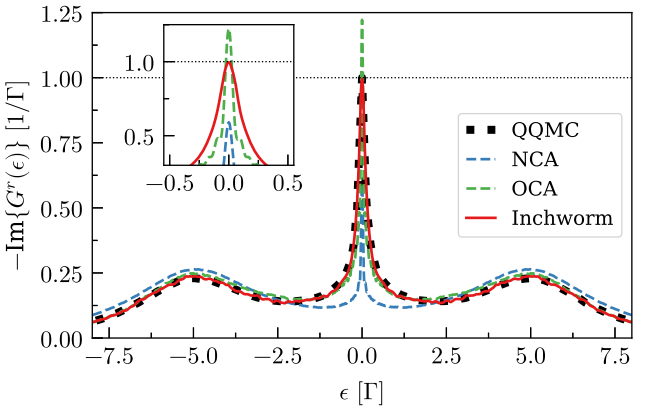

FIG. 2. Steady-state spectral function in the Kondo regime. The bath consists of a single semielliptic band $\Gamma(\epsilon) = \frac{\Gamma}{\Delta}\sqrt{\Delta^2 - \epsilon^2}$ at $\mu = 0$, where $|\epsilon| < \Delta$, with $\Delta = 11.476\Gamma$. Parameters are particle-hole symmetric with $U = -2\epsilon_0 = 8\Gamma$, the temperature is $T = 10^{-8}\Gamma$. The IQMC scheme converges at order 15 (9) for the propagator (GF). QQMC data are extracted from Ref. [93]. Inset: low energies and Kondo resonance.

orders, together with the analytic result. The noncrossing approximation (NCA) and one-crossing approximation (OCA) represent the lowest and next-to-lowest order truncation of the inchworm hybridization expansion [66,86–91]. When beyond-OCA diagrams are added, the propagator (not shown) stabilizes at fourth order, in the sense that including higher orders does not alter the results within the Monte Carlo error. In the same sense, the GFs stabilize at sixth order. The data are consistent with the exact result to within the Monte Carlo error. A time-dependent IQMC calculation [51,92] using the same numerical parameters would have a computational cost approximately ∼1000 times larger, not including the time needed to overcome the transient dynamics from a known initial state.

Benchmarks II: Kondo regime.—Providing an accurate description of Kondo physics is a paradigmatic benchmark for methods applicable to correlated systems. In Fig. 2, we consider parameters that were recently studied using two state-of-the-art algorithms: the quantum quasi-Monte Carlo (QQMC) [93,94] and the fork tensor product state (FTPS) [95] methods. We compare the spectral function of the Anderson impurity model in the Kondo regime, as calculated by the steady-state IQMC method, to the QQMC data provided in Ref. [93] and validated there against the FTPS method. With our implementation, the computational cost for the steady-state IQMC result is ∼10000 core hours. While this might be a daunting number for many types of numerical methods, the fact that Monte Carlo simulations are extremely parallelizable makes it entirely manageable and is a crucial element in their appeal. The agreement between the data is very good, yet the principles underlying the two methods are very different: QQMC is an interaction expansion while IQMC is a hybridization expansion; and the IQMC method entails fewer assumptions regarding the analytical structure of the problem and the properties of the integrand characterizing the expansion. The spectral function exhibits a sharp Kondo peak at the Fermi level and two Hubbard bands centered around $\epsilon \sim \pm U/2$. Within Monte Carlo errors, the IQMC data reproduce the Friedel sum rule $\mathrm{Im}[G^r(\epsilon = 0)] = -1/\Gamma$ [96] and resolve the low energy frequency dependence well (see inset of Fig. 2). These features and the associated physical interpretation as well as the temperature dependence of the Kondo resonance are discussed in the literature [96–98]. In contrast, while the NCA and OCA capture the main features, they fail to provide quantitative results, especially at low energies.

Equilibrium DMFT.—Interacting lattice models can be mapped self-consistently onto effective impurity models with DMFT [52,56,99,100]. The method is in general approximate, but becomes exact for the infinite coordination number Bethe lattice [52]. In order to contrast the spectral features of an impurity with that of a correlated material, we consider three different scenarios: (i) an impurity coupled to two noninteracting leads, (ii) an isolated Bethe lattice in the infinite coordination number limit, describing a correlated material in equilibrium [101–103], and (iii) an infinite-coordination Bethe lattice coupled to two noninteracting leads, describing a correlated material in a junction [56,58,104,105]. Additional details on the simulation setup for these scenarios are provided in the Supplemental Material [83].

Figure 3 presents IQMC results for the equilibrium spectral functions for these three scenarios at different temperatures. The computational cost for the steady-state IQMC result ranges from ∼1000 core hours per DMFT iteration for higher temperatures to ∼10000 core hours per

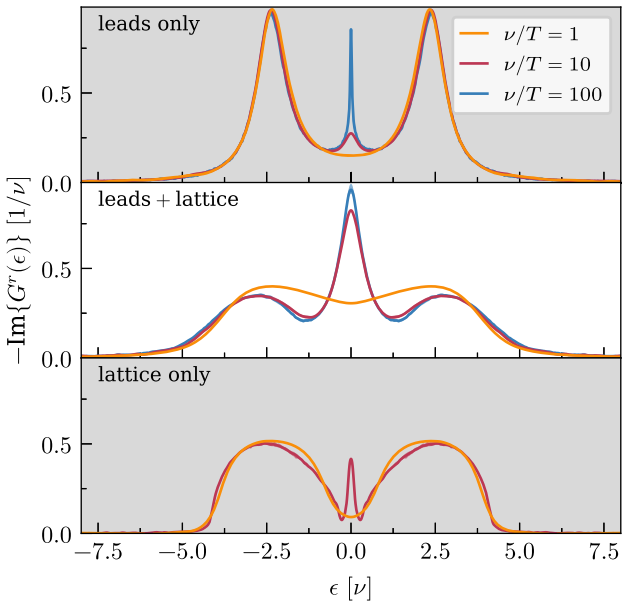

FIG. 3. Interacting local equilibrium spectral function at different temperatures for an impurity coupled to leads (top), an isolated correlated material (bottom), and a correlated material coupled to leads (middle). The material is modeled as an infinite-dimensional Bethe lattice with intersite hopping ν, which we use as the overall energy scale; other parameters are $U = -2\epsilon_0 = 4.6\nu$. The leads are parametrized by wide, flat bands with smooth cutoffs: $\Gamma_\ell(\epsilon) = \Gamma/[(1 + e^{\eta[(\epsilon-\mu_\ell)-\omega_c]})(1 + e^{-\eta[(\epsilon-\mu_\ell)+\omega_c]})]$, with $\Gamma = 0.125\nu, \eta = 10/\nu, \omega_c = 10\nu, \mu_\ell = 0$, and $\ell \in \{L, R\}$. To estimate the error, we plot the average and the standard deviation of three consecutive DMFT iterations (middle and bottom panel), where typical errors are of the size $3 \times 10^{-2}/\nu$.

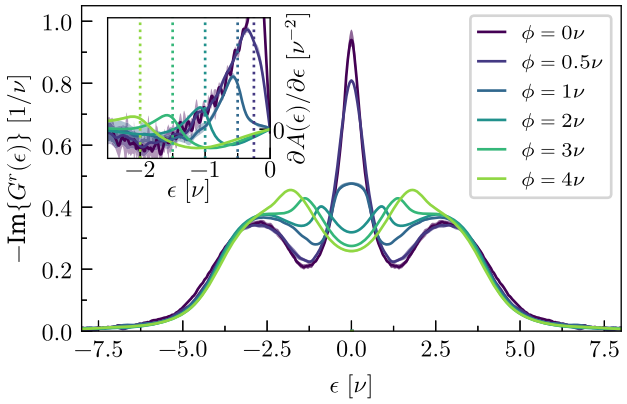

FIG. 4. Nonequilibrium spectral function for a correlated material in a junction for different bias voltages ϕ. The parameters are as in the middle panel of Fig. 3, with temperature $T = \nu/100$. The average and the standard deviation of three consecutive DMFT iterations are shown to provide an error estimate, where typical errors are of the size $3 \times 10^{-2}/\nu$. Inset: derivative of the spectral function with respect to energy. Vertical dashed lines show value of the chemical potential in the right lead.

DMFT iteration for the correlated regime. The equilibrium behavior of scenarios (i) and (ii) is well established [52,57,96–99] and serves to rationalize the behavior of system (iii). All three systems exhibit a coherence peak at the Fermi energy at low temperatures, and two Hubbard bands centered around $\epsilon \simeq \pm U/2$. In all cases, increasing the temperature results in the melting of the coherence peak and a redistribution of its spectral weight to higher energies. In the impurity case (top panel), features are sharpened by a relatively weak coupling to the leads. In the isolated lattice (bottom panel), features are more rounded, but the band edge is sharper. This case is analogous to standard (usually imaginary time) DMFT calculations, and we have validated our results against numerically exact imaginary-time Monte Carlo data (not shown) [106]. Finally, the lattice coupled to a junction exhibits the most pronounced correlation effect, since the effective impurity couples to both the correlated lattice and the leads, and as a result has a higher Kondo temperature [96]. Its dependence on temperature can be explained based on this increased coupling.

Nonequilibrium DMFT.—The infinite-coordination Bethe lattice coupled to leads can be driven away from equilibrium by applying a bias voltage $\phi = \mu_L - \mu_R$ between the two leads, making them an electronic junction. We apply a symmetric bias voltage, $\mu_L = -\mu_R$. The model remains exactly solvable by way of nonequilibrium DMFT [55–57]. Previous studies of similar systems were restricted to approximate impurity solvers [58,104,105,107,108].

Figure 4 shows the spectral function at different bias voltages ϕ, with $\phi = 0$ corresponding to the equilibrium case in Fig. 3. At low bias $\phi \lesssim 1\nu$, we observe a shrinking of the quasiparticle peak and a formation of a plateau centered around $\epsilon = 0$, with its width determined by ϕ; peaks in the derivative of the spectral function with respect to energy appear at $\epsilon \approx \mu_{L/R}$ (see inset in Fig. 4). At higher bias, $\phi \gtrsim 2\nu$, the peak splits into two short peaks centered at $\epsilon = \mu_{L/R}$, which are narrower than half the width of the plateau. The splitting is as one would expect in quantum dot junctions [59,62–66,69,109–113]. The formation of the plateau at intermediate values of ϕ indicates that the correlated material stabilizes its equivalent of the Kondo resonance and pins it to the equilibrium chemical potential, a mechanism not present in quantum dot junctions. We note that the plateau formation is not visible in low-order calculations like the NCA (data not shown). We speculate that it results from the interplay between several correlation features: two correlation peaks pinned to the changing chemical potentials of the leads, and a central peak remaining at energy zero and associated with Kondo physics within the Bethe lattice. The latter is suppressed when the bias voltage is increased, due to reduced hybridization at zero energy when the other two peaks are shifted, as well as an increased effective temperature in the lattice. This eventually destroys the plateau at high enough bias. To our knowledge, the plateau effect has not been previously predicted, and obtaining a full theoretical

understanding of its mechanism remains an open challenge. As we find this effect in a model where each lattice site is coupled to its neighbors and to two leads, we expect that the plateau effect is observable in experiments where this setup is essentially realized. We hypothesize that the plateau effect can be observed in transport measurements on quasi-two-dimensional or thin-film correlated materials [3,114], layered moiré systems [115,116], and multiple-quantum-dot systems out of equilibrium [117–119]. The corresponding findings will be indicative for the behavior and the interplay of different correlation effects in nonequilibrium.

Conclusion.—We presented a Monte Carlo method for quantum impurity models that is formulated directly in the steady state and is applicable in and out of equilibrium. The method, which is based on the inchworm hybridization expansion, can be used to describe transport through quantum dot junctions directly, and strongly correlated materials by way of the DMFT. Our formulation utilizes the fact that the two-time structure of restricted propagators on the Keldysh contour can be reduced to a time-difference representation in the steady state, which enables their evaluation at a computational cost that is expected to scale linearly with the coherence time of the system. The scheme then provides a self-consistency condition for the restricted propagators, which is solved iteratively. We implemented and benchmarked the method for the Anderson impurity model and showed that it can be used to describe a strongly correlated material using DMFT, providing real frequency data without resorting to analytical continuation. We then investigated a correlated material in a junction between two metallic leads and driven out of equilibrium by a bias voltage. We found a bias-induced splitting of the quasiparticle peak, which occurs at higher voltages than one might expect from our understanding of transport through quantum dots, and which is preceded by the formation of a spectral plateau. Our method promises to enable the numerically exact treatment of a wide variety of problems spanning quantum transport, equilibrium materials science, and novel types of strongly correlated nonequilibrium effects that are of experimental interest.

We thank J. Kleinhenz and Y. Yu for helpful discussions. A. E. was funded by the Deutsche Forschungsgemeinschaft (DFG, German Research Foundation)—453644843, and by the Raymond and Beverly Sackler Center for Computational Molecular and Materials Science, Tel Aviv University. The work of E. G. was supported by the U.S. Department of Energy, Office of Science, Office of Advanced Scientific Computing Research and Office of Basic Energy Sciences, Scientific Discovery through Advanced Computing (SciDAC) program under Award No. DE-SC0022088. This research used resources of the National Energy Research Scientific Computing Center, a DOE Office of Science User Facility supported by the Office of Science of the U.S. Department of Energy under Contract No. DE-AC02-05CH11231 using NERSC award BES-ERCAP0021805. G. C. acknowledges support by the Israel Science Foundation (Grants No. 2902/21 and No. 218/19) and by the PAZY foundation (Grant No. 318/78).

[1] G. Stefanovich, A. Pergament, and D. Stefanovich, J. Phys. Condens. Matter **12**, 8837 (2000).
[2] H.-T. Kim, B.-G. Chae, D.-H. Youn, S.-L. Maeng, G. Kim, K.-Y. Kang, and Y.-S. Lim, New J. Phys. **6**, 52 (2004).
[3] S. Guénon, S. Scharinger, S. Wang, J. G. Ramírez, D. Koelle, R. Kleiner, and I. K. Schuller, Europhys. Lett. **101**, 57003 (2013).
[4] P. Stoliar, L. Cario, E. Janod, B. Corraze, C. Guillot-Deudon, S. Salmon-Bourmand, V. Guiot, J. Tranchant, and M. Rozenberg, Adv. Mater. **25**, 3222 (2013).
[5] J. S. Brockman, L. Gao, B. Hughes, C. T. Rettner, M. G. Samant, K. P. Roche, and S. S. Parkin, Nat. Nanotechnol. **9**, 453 (2014).
[6] J. Del Valle, P. Salev, F. Tesler, N. M. Vargas, Y. Kalcheim, P. Wang, J. Trastoy, M.-H. Lee, G. Kassabian, J. G. Ramírez *et al.*, Nature (London) **569**, 388 (2019).
[7] J. del Valle, N. M. Vargas, R. Rocco, P. Salev, Y. Kalcheim, P. N. Lapa, C. Adda, M.-H. Lee, P. Y. Wang, L. Fratino, M. J. Rozenberg, and I. K. Schuller, Science **373**, 907 (2021).
[8] J. del Valle, R. Rocco, C. Domínguez, J. Fowlie, S. Gariglio, M. J. Rozenberg, and J.-M. Triscone, Phys. Rev. B **104**, 165141 (2021).
[9] T. Ogasawara, M. Ashida, N. Motoyama, H. Eisaki, S. Uchida, Y. Tokura, H. Ghosh, A. Shukla, S. Mazumdar, and M. Kuwata-Gonokami, Phys. Rev. Lett. **85**, 2204 (2000).
[10] L. Stojchevska, I. Vaskivskyi, T. Mertelj, P. Kusar, D. Svetin, S. Brazovskii, and D. Mihailovic, Science **344**, 177 (2014).
[11] J. Zhang, X. Tan, M. Liu, S. W. Teitelbaum, K. W. Post, F. Jin, K. A. Nelson, D. N. Basov, W. Wu, and R. D. Averitt, Nat. Mater. **15**, 956 (2016).
[12] M. P. Dean, Y. Cao, X. Liu, S. Wall, D. Zhu, R. Mankowsky, V. Thampy, X. Chen, J. G. Vale, D. Casa *et al.*, Nat. Mater. **15**, 601 (2016).
[13] D. Fausti, R. I. Tobey, N. Dean, S. Kaiser, A. Dienst, M. C. Hoffmann, S. Pyon, T. Takayama, H. Takagi, and A. Cavalleri, Science **331**, 189 (2011).
[14] D. Nicoletti, E. Casandruc, Y. Laplace, V. Khanna, C. R. Hunt, S. Kaiser, S. S. Dhesi, G. D. Gu, J. P. Hill, and A. Cavalleri, Phys. Rev. B **90**, 100503(R) (2014).
[15] M. Mitrano, A. Cantaluppi, D. Nicoletti, S. Kaiser, A. Perucchi, S. Lupi, P. Di Pietro, D. Pontiroli, M. Riccò, S. R. Clark *et al.*, Nature (London) **530**, 461 (2016).
[16] C. Bao, P. Tang, D. Sun, and S. Zhou, Nat. Rev. Phys. **4**, 33 (2022).
[17] H. Takagi and H. Y. Hwang, Science **327**, 1601 (2010).
[18] S. Iwai, M. Ono, A. Maeda, H. Matsuzaki, H. Kishida, H. Okamoto, and Y. Tokura, Phys. Rev. Lett. **91**, 057401 (2003).

[19] L. Perfetti, P. A. Loukakos, M. Lisowski, U. Bovensiepen, H. Berger, S. Biermann, P. S. Cornaglia, A. Georges, and M. Wolf, Phys. Rev. Lett. **97**, 067402 (2006).

[20] S. Wall, D. Brida, S. R. Clark, H. P. Ehrke, D. Jaksch, A. Ardavan, S. Bonora, H. Uemura, Y. Takahashi, T. Hasegawa *et al.*, Nat. Phys. **7**, 114 (2011).

[21] N. Dean, J. C. Petersen, D. Fausti, R. I. Tobey, S. Kaiser, L. V. Gasparov, H. Berger, and A. Cavalleri, Phys. Rev. Lett. **106**, 016401 (2011).

[22] H. Ichikawa, S. Nozawa, T. Sato, A. Tomita, K. Ichiyanagi, M. Chollet, L. Guerin, N. Dean, A. Cavalleri, S.-i. Adachi *et al.*, Nat. Mater. **10**, 101 (2011).

[23] S. H. Dietze, M. J. Marsh, S. Wang, J.-G. Ramírez, Z.-H. Cai, J. R. Mohanty, I. K. Schuller, and O. G. Shpyrko, Phys. Rev. B **90**, 165109 (2014).

[24] T. Konstantinova, J. D. Rameau, A. H. Reid, O. Abdurazakov, L. Wu, R. Li, X. Shen, G. Gu, Y. Huang, L. Rettig, I. Avigo, M. Ligges, J. K. Freericks, A. F. Kemper, H. A. Dürr, U. Bovensiepen, P. D. Johnson, X. Wang, and Y. Zhu, Sci. Adv. **4**, eaap7427 (2018).

[25] A. Ronchi, P. Homm, M. Menghini, P. Franceschini, F. Maccherozzi, F. Banfi, G. Ferrini, F. Cilento, F. Parmigiani, S. S. Dhesi, M. Fabrizio, J.-P. Locquet, and C. Giannetti, Phys. Rev. B **100**, 075111 (2019).

[26] S. M. Cronenwett, H. J. Lynch, D. Goldhaber-Gordon, L. P. Kouwenhoven, C. M. Marcus, K. Hirose, N. S. Wingreen, and V. Umansky, Phys. Rev. Lett. **88**, 226805 (2002).

[27] P. Limelette, A. Georges, D. Jérome, P. Wzietek, P. Metcalf, and J. Honig, Science **302**, 89 (2003).

[28] F. Kagawa, T. Itou, K. Miyagawa, and K. Kanoda, Phys. Rev. B **69**, 064511 (2004).

[29] S. Lee, A. Fursina, J. T. Mayo, C. T. Yavuz, V. L. Colvin, R. Sumesh Sofin, I. V. Shvets, and D. Natelson, Nat. Mater. **7**, 130 (2008).

[30] J. del Valle, Y. Kalcheim, J. Trastoy, A. Charnukha, D. N. Basov, and I. K. Schuller, Phys. Rev. Appl. **8**, 054041 (2017).

[31] J. C. Gonzalez-Rosillo, S. Catalano, I. Maggio-Aprile, M. Gibert, X. Obradors, A. Palau, and T. Puig, Small **16**, 2001307 (2020).

[32] D. Hou, R. Wang, X. Zheng, N. H. Tong, J. H. Wei, and Y. J. Yan, Phys. Rev. B **90**, 045141 (2014).

[33] A. Erpenbeck, C. Hertlein, and C. Schinabeck, and M. Thoss, J. Chem. Phys. **149**, 064106 (2018).

[34] H.-D. Zhang, L. Cui, H. Gong, R.-X. Xu, X. Zheng, and Y. Yan, J. Chem. Phys. **152**, 064107 (2020).

[35] Z.-H. Chen, Y. Wang, X. Zhen, R.-X. Xu, and Y. Yan, J. Chem. Phys. **156**, 221102 (2022).

[36] K. Balzer, Z. Li, O. Vendrell, and M. Eckstein, Phys. Rev. B **91**, 045136 (2015).

[37] F. Schwarz, I. Weymann, J. von Delft, and A. Weichselbaum, Phys. Rev. Lett. **121**, 137702 (2018).

[38] M. Lotem, A. Weichselbaum, J. von Delft, and M. Goldstein, Phys. Rev. Res. **2**, 043052 (2020).

[39] P. Nordlander, M. Pustilnik, Y. Meir, N. S. Wingreen, and D. C. Langreth, Phys. Rev. Lett. **83**, 808 (1999).

[40] E. Gull, D. R. Reichman, and A. J. Millis, Phys. Rev. B **84**, 085134 (2011).

[41] G. Cohen, E. Gull, D. R. Reichman, A. J. Millis, and E. Rabani, Phys. Rev. B **87**, 195108 (2013).

[42] S. R. White and A. E. Feiguin, Phys. Rev. Lett. **93**, 076401 (2004).

[43] G. Vidal, Phys. Rev. Lett. **93**, 040502 (2004).

[44] A. J. Daley, C. Kollath, U. Schollwöck, and G. Vidal, J. Stat. Mech. (2004) P04005.

[45] F. B. Anders and A. Schiller, Phys. Rev. Lett. **95**, 196801 (2005).

[46] Y. Tanimura, J. Phys. Soc. Jpn. **75**, 082001 (2006).

[47] S. Welack, M. Schreiber, and U. Kleinekathöfer, J. Chem. Phys. **124**, 044712 (2006).

[48] J. Jin, X. Zheng, and Y. Yan, J. Chem. Phys. **128**, 234703 (2008).

[49] R. Härtle, G. Cohen, D. R. Reichman, and A. J. Millis, Phys. Rev. B **88**, 235426 (2013).

[50] R. Härtle, G. Cohen, D. R. Reichman, and A. J. Millis, Phys. Rev. B **92**, 085430 (2015).

[51] G. Cohen, E. Gull, D. R. Reichman, and A. J. Millis, Phys. Rev. Lett. **115**, 266802 (2015).

[52] A. Georges, G. Kotliar, W. Krauth, and M. J. Rozenberg, Rev. Mod. Phys. **68**, 13 (1996).

[53] M. Jarrell and J. Gubernatis, Phys. Rep. **269**, 133 (1996).

[54] J. Fei, C.-N. Yeh, and E. Gull, Phys. Rev. Lett. **126**, 056402 (2021).

[55] J. K. Freericks, V. M. Turkowski, and V. Zlatić, Phys. Rev. Lett. **97**, 266408 (2006).

[56] H. Aoki, N. Tsuji, M. Eckstein, M. Kollar, T. Oka, and P. Werner, Rev. Mod. Phys. **86**, 779 (2014).

[57] V. Turkowski, Nonequilibrium DMFT, in *Dynamical Mean-Field Theory for Strongly Correlated Materials* (Springer International Publishing, Cham, 2021), pp. 223–272.

[58] E. Arrigoni, M. Knap, and W. von der Linden, Phys. Rev. Lett. **110**, 086403 (2013).

[59] Y. Meir, N. S. Wingreen, and P. A. Lee, Phys. Rev. Lett. **70**, 2601 (1993).

[60] N. S. Wingreen and Y. Meir, Phys. Rev. B **49**, 11040 (1994).

[61] E. Lebanon and A. Schiller, Phys. Rev. B **65**, 035308 (2001).

[62] S. De Franceschi, R. Hanson, W. G. van der Wiel, J. M. Elzerman, J. J. Wijpkema, T. Fujisawa, S. Tarucha, and L. P. Kouwenhoven, Phys. Rev. Lett. **89**, 156801 (2002).

[63] R. Leturcq, L. Schmid, K. Ensslin, Y. Meir, D. C. Driscoll, and A. C. Gossard, Phys. Rev. Lett. **95**, 126603 (2005).

[64] N. Shah and A. Rosch, Phys. Rev. B **73**, 081309(R) (2006).

[65] P. Fritsch and S. Kehrein, Phys. Rev. B **81**, 035113 (2010).

[66] G. Cohen, D. R. Reichman, A. J. Millis, and E. Gull, Phys. Rev. B **89**, 115139 (2014).

[67] G. Cohen, E. Gull, D. R. Reichman, and A. J. Millis, Phys. Rev. Lett. **112**, 146802 (2014).

[68] T.-F. Fang, A.-M. Guo, and Q.-F. Sun, Phys. Rev. B **97**, 235115 (2018).

[69] I. Krivenko, J. Kleinhenz, G. Cohen, and E. Gull, Phys. Rev. B **100**, 201104(R) (2019).

[70] A. Erpenbeck and G. Cohen, SciPost Phys. **10**, 142 (2021).

[71] L. Mühlbacher and E. Rabani, Phys. Rev. Lett. **100**, 176403 (2008).

[72] P. Werner, T. Oka, and A. J. Millis, Phys. Rev. B **79**, 035320 (2009).

[73] M. Schiró and M. Fabrizio, Phys. Rev. B **79**, 153302 (2009).
[74] E. Gull, A. J. Millis, A. I. Lichtenstein, A. N. Rubtsov, M. Troyer, and P. Werner, Rev. Mod. Phys. **83**, 349 (2011).
[75] M. Schiró, Phys. Rev. B **81**, 085126 (2010).
[76] E. Gull, D. R. Reichman, and A. J. Millis, Phys. Rev. B **82**, 075109 (2010).
[77] A. E. Antipov, Q. Dong, and E. Gull, Phys. Rev. Lett. **116**, 036801 (2016).
[78] A. E. Antipov, Q. Dong, J. Kleinhenz, G. Cohen, and E. Gull, Phys. Rev. B **95**, 085144 (2017).
[79] H.-T. Chen, G. Cohen, and D. R. Reichman, J. Chem. Phys. **146**, 054105 (2017).
[80] H.-T. Chen, G. Cohen, and D. R. Reichman, J. Chem. Phys. **146**, 054106 (2017).
[81] Z. Cai, J. Lu, and S. Yang, Commun. Pure Appl. Math. **73**, 2430 (2020).
[82] Z. Cai, J. Lu, and S. Yang, arXiv:2006.07654.
[83] See Supplemental Material at http://link.aps.org/supplemental/10.1103/PhysRevLett.130.186301 for detailed derivation and technical details.
[84] H. Bruus and K. Flensberg, *Many-Body Quantum Theory in Condensed Matter Physics: An Introduction*, Oxford Graduate Texts (Oxford University Press, Oxford, 2004).
[85] H. J. W. Haug and A.-P. Jauho, *Quantum Kinetics in Transport and Optics of Semiconductors*, Springer Series in Solid-State Sciences (Springer, Berlin, 2008).
[86] N. E. Bickers, Rev. Mod. Phys. **59**, 845 (1987).
[87] T. Pruschke and N. Grewe, Z. Phys. B Condens. Matter **74**, 439 (1989).
[88] T. Pruschke, D. L. Cox, and M. Jarrell, Phys. Rev. B **47**, 3553 (1993).
[89] K. Haule, S. Kirchner, J. Kroha, and P. Wölfle, Phys. Rev. B **64**, 155111 (2001).
[90] M. Eckstein and P. Werner, Phys. Rev. B **82**, 115115 (2010).
[91] A. Erpenbeck, E. Gull, and G. Cohen, Phys. Rev. B **103**, 125431 (2021).
[92] A. Boag, E. Gull, and G. Cohen, Phys. Rev. B **98**, 115152 (2018).
[93] C. Bertrand, D. Bauernfeind, P. T. Dumitrescu, M. Maček, X. Waintal, and O. Parcollet, Phys. Rev. B **103**, 155104 (2021).
[94] M. Maček, P. T. Dumitrescu, C. Bertrand, B. Triggs, O. Parcollet, and X. Waintal, Phys. Rev. Lett. **125**, 047702 (2020).
[95] D. Bauernfeind, M. Zingl, R. Triebl, M. Aichhorn, and H. G. Evertz, Phys. Rev. X **7**, 031013 (2017).
[96] A. Hewson and D. Edwards, *The Kondo Problem to Heavy Fermions*, Cambridge Studies in Magnetism (Cambridge University Press, Cambridge, England, 1997).
[97] P. W. Anderson, J. Phys. C **3**, 2436 (1970).
[98] J. R. Schrieffer and P. A. Wolff, Phys. Rev. **149**, 491 (1966).
[99] D. Vollhardt, K. Byczuk, and M. Kollar, Dynamical mean-field theory, in *Strongly Correlated Systems: Theoretical Methods*, edited by A. Avella and F. Mancini (Springer, Berlin, 2012).
[100] D. Vollhardt, Ann. Phys. (Berlin) **524**, 1 (2012).
[101] W. Metzner and D. Vollhardt, Phys. Rev. Lett. **62**, 324 (1989).
[102] E. Müller-Hartmnn, Z. Phys. B **74**, 507 (1989).
[103] A. Georges and G. Kotliar, Phys. Rev. B **45**, 6479 (1992).
[104] S. Okamoto, Phys. Rev. Lett. **101**, 116807 (2008).
[105] J. Kleinhenz, I. Krivenko, G. Cohen, and E. Gull, Phys. Rev. B **102**, 205138 (2020).
[106] E. Gull, P. Werner, O. Parcollet, and M. Troyer, Europhys. Lett. **82**, 57003 (2008).
[107] N. Tsuji and P. Werner, Phys. Rev. B **88**, 165115 (2013).
[108] I. Titvinidze, A. Dorda, W. von der Linden, and E. Arrigoni, Phys. Rev. B **92**, 245125 (2015).
[109] J. E. Han and R. J. Heary, Phys. Rev. Lett. **99**, 236808 (2007).
[110] F. B. Anders, Phys. Rev. Lett. **101**, 066804 (2008).
[111] A. Dorda, M. Ganahl, H. G. Evertz, W. von der Linden, and E. Arrigoni, Phys. Rev. B **92**, 125145 (2015).
[112] D. M. Fugger, A. Dorda, F. Schwarz, J. von Delft, and E. Arrigoni, New J. Phys. **20**, 013030 (2018).
[113] D. M. Fugger, D. Bauernfeind, M. E. Sorantin, and E. Arrigoni, Phys. Rev. B **101**, 165132 (2020).
[114] H. J. Harsan Ma, S. Scharinger, S. W. Zeng, D. Kohlberger, M. Lange, A. Stöhr, X. R. Wang, T. Venkatesan, R. Kleiner, J. F. Scott, J. M. D. Coey, D. Koelle, and Ariando, Phys. Rev. Lett. **116**, 257601 (2016).
[115] Nat. Rev. Mater. **6**, 191 (2021).
[116] Y. Zhou, D. N. Sheng, and E.-A. Kim, Phys. Rev. Lett. **128**, 157602 (2022).
[117] P. Barthelemy and L. M. K. Vandersypen, Ann. Phys. (Amsterdam) **525**, 808 (2013).
[118] A. Keller, L. Peeters, C. Moca, I. Weymann, D. Mahalu, V. Umansky, G. Zaránd, and D. Goldhaber-Gordon, Nature (London) **526**, 237 (2015).
[119] W. Pouse, L. Peeters, C. L. Hsueh, U. Gennser, A. Cavanna, M. A. Kastner, A. K. Mitchell, and D. Goldhaber-Gordon, Nat. Phys. **19**, 492 (2023).